## Supplemental Information

# Intestinal CYP3A4 protects against lithocholic acid-induced hepatotoxicity in vitamin D receptor intestine-deficient mice

Jie Cheng, Zhong-Ze Fang, Jung-Hwan Kim, Kristopher W. Krausz, Naoki Tanaka, John Y.L. Chiang, and Frank J. Gonzalez

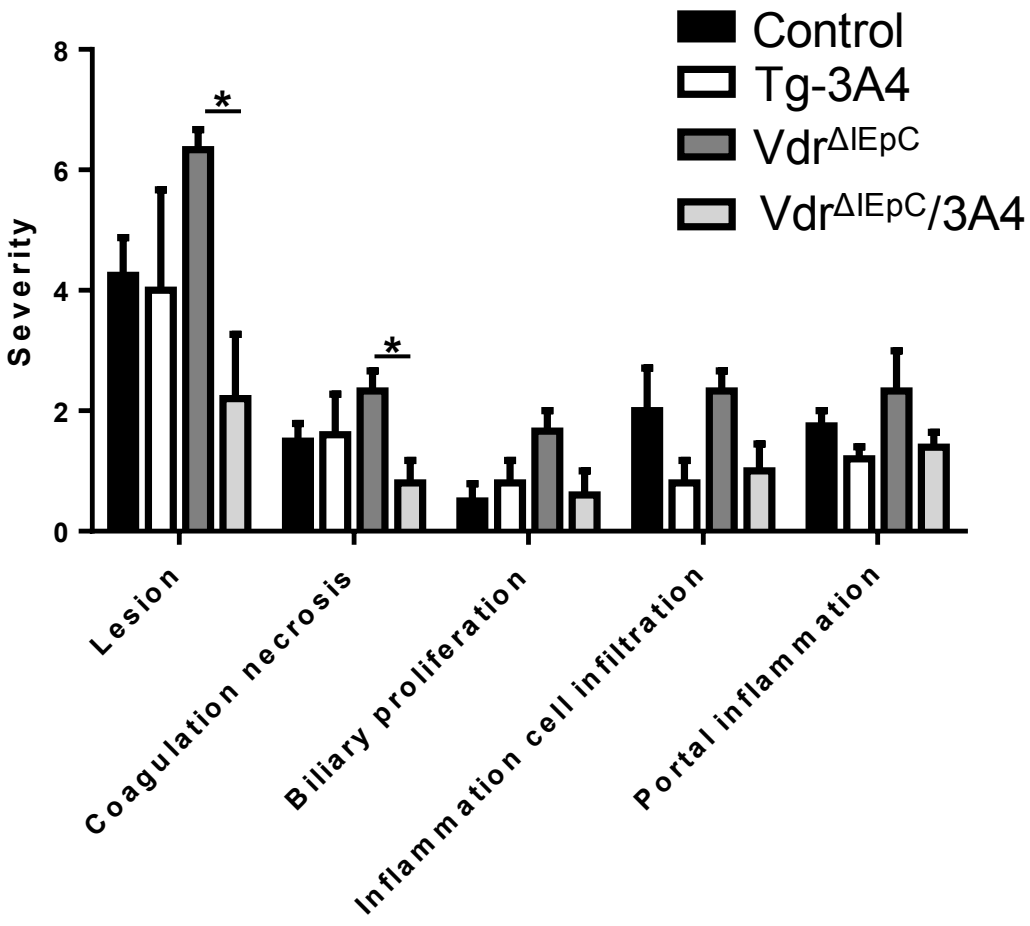


**Supplemental Figure 1.** Scoring of histological liver damage. The lesion score was defined as the proportion of the liver affected relative to the total area of liver section, and presented on an ordinal scale 1 to 10. Coagulation necrosis originates adjacent to the portal tract and extending to midzonal and centrilobular regions was associated with variable congestion. Biliary proliferation is the increased numbers of variably basophilic bile ducts and biliary epithelial cells.

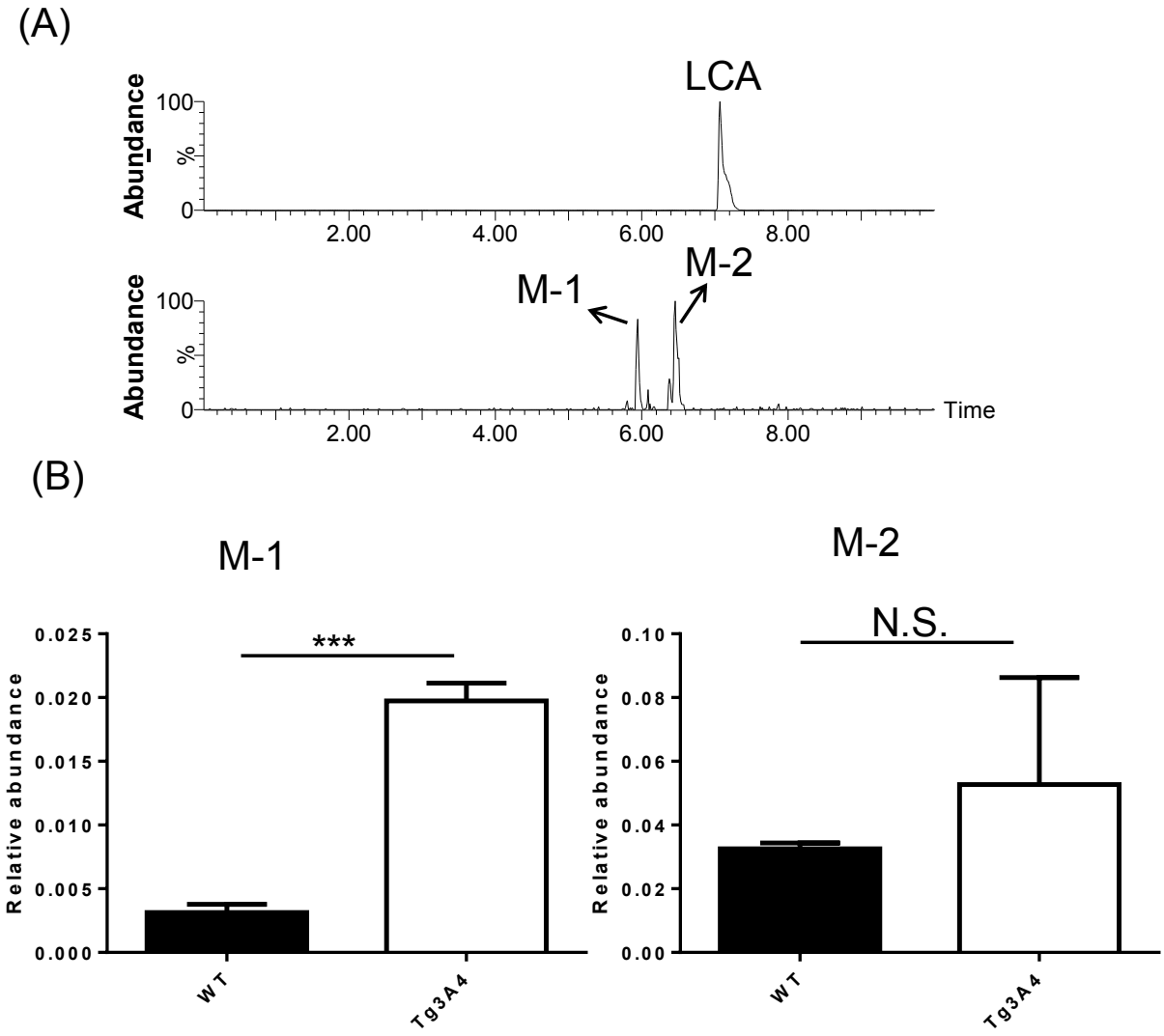


**Supplemental Figure 2.** Comparison the hydroxylation reaction of LCA. The negative mode was used to monitor LCA ($[M-H]^-$=375.290) and its hydroxylated products ($[M-H]^-$=391.285). (A) Respective chromatography figure of LCA and its hydroxylated products. Two hydroxylated products were detected, and referred as LCA-OH-1 and LCA-OH-2. (B) The relative abundance of LCA-OH-1 and LCA-OH-2 in WT and Tg3A4 incubation system. The data were given as mean±S.D. (N=4). ***, $p<0.001$; N.S., not significant.

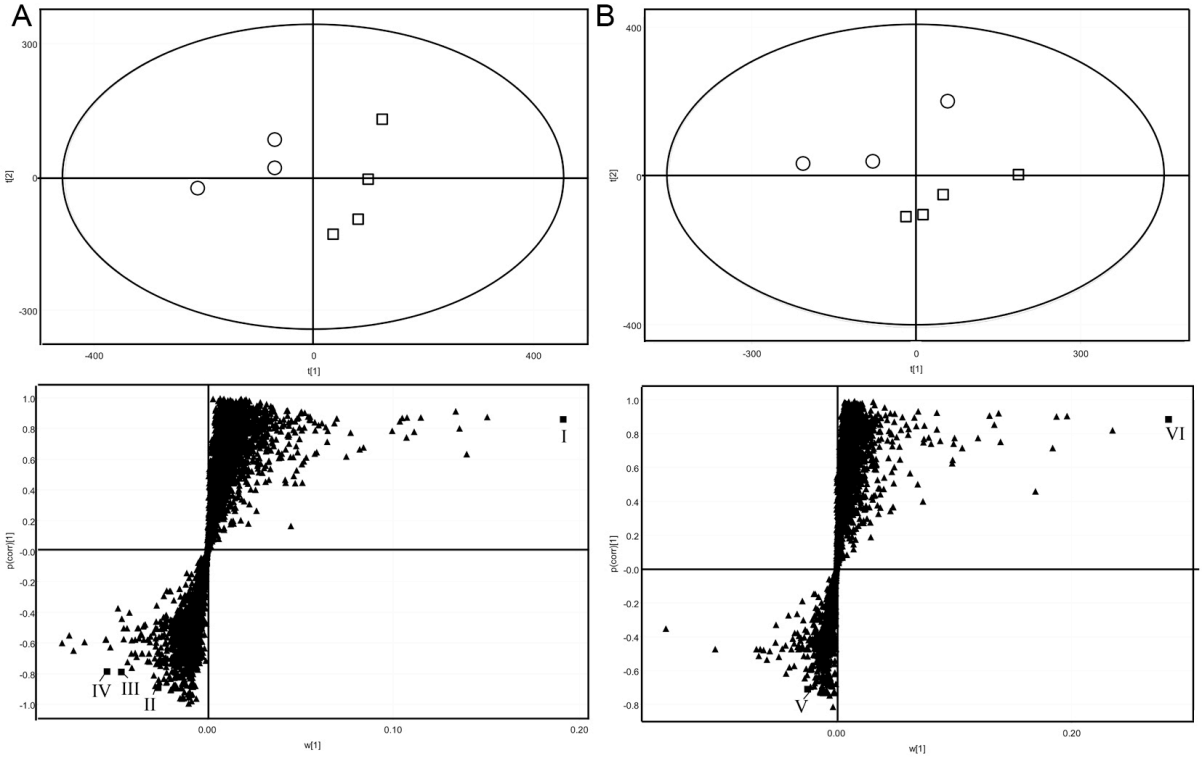


**Supplemental Figure. 3.** Metabolomics analysis of urine in positive mode from *Vdr*$^{\Delta IEpC}$ and *Vdr*$^{\Delta IEpC}$/3A4 mice treated with LCA. A. PLS-DA analysis (upper panel A) of the positive urinary metabolome revealed a clear separation of *Vdr*$^{\Delta IEpC}$ (□) and *Vdr*$^{\Delta IEpC}$/3A4 (○). Loading plots (Lower panel A) from the PCA analysis of urinary metabolomes showing LCA and LCA metabolites labeled with boxes: I (377.146$^{+}$), II (393.133$^{+}$), III (434.313$^{+}$), and IV (553.697$^{+}$) contributing to the distinctive clustering of *Vdr*$^{\Delta IEpC}$ and *Vdr*$^{\Delta IEpC}$/3A4 mice. B. PLSDA analysis (upper panel B) of the negative urinary metabolome revealed a clear separation of *Vdr*$^{\Delta IEpC}$ (□) and *Vdr*$^{\Delta IEpC}$/3A4 (○). Loading plots (lower panel B) from the PCA analysis of urinary metabolomes showing LCA metabolites and other biomarkers labeled with boxes: V (481.31$^{-}$), and IV (124.141$^{-}$). Metabolites are identified as I: lithocholic acid, II: hydroxylated lithocholic acid, III: lithocholic acid glycine conjugate, IV: lithocholate-O-glucuronide, V: lithocholyltaurine and VI: taurine respectively by comparison with the authentic standard or through MSMS fragmentation and structure identification.

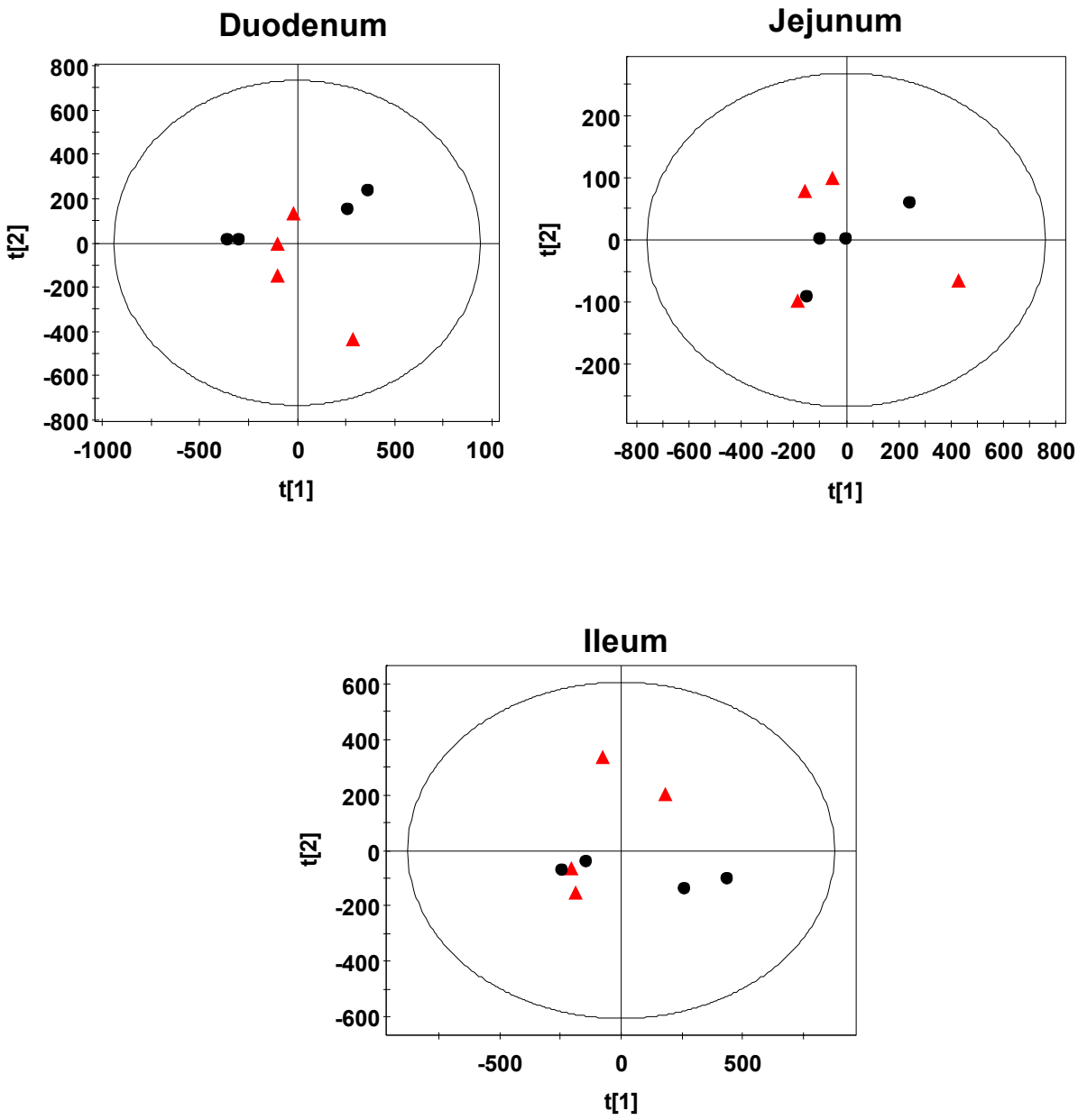


**Supplemental Figure 4.** Metabolomics analysis of intestine (duodenum, jejunum, and ileum) homogenates in wild-type and Tg-3A4 mice. PCA scores scatter plot for intestine (duodenum, jejunum, and ileum) homogenates of wild type (●) and Tg-3A4 (▲) mice under the negative mode.

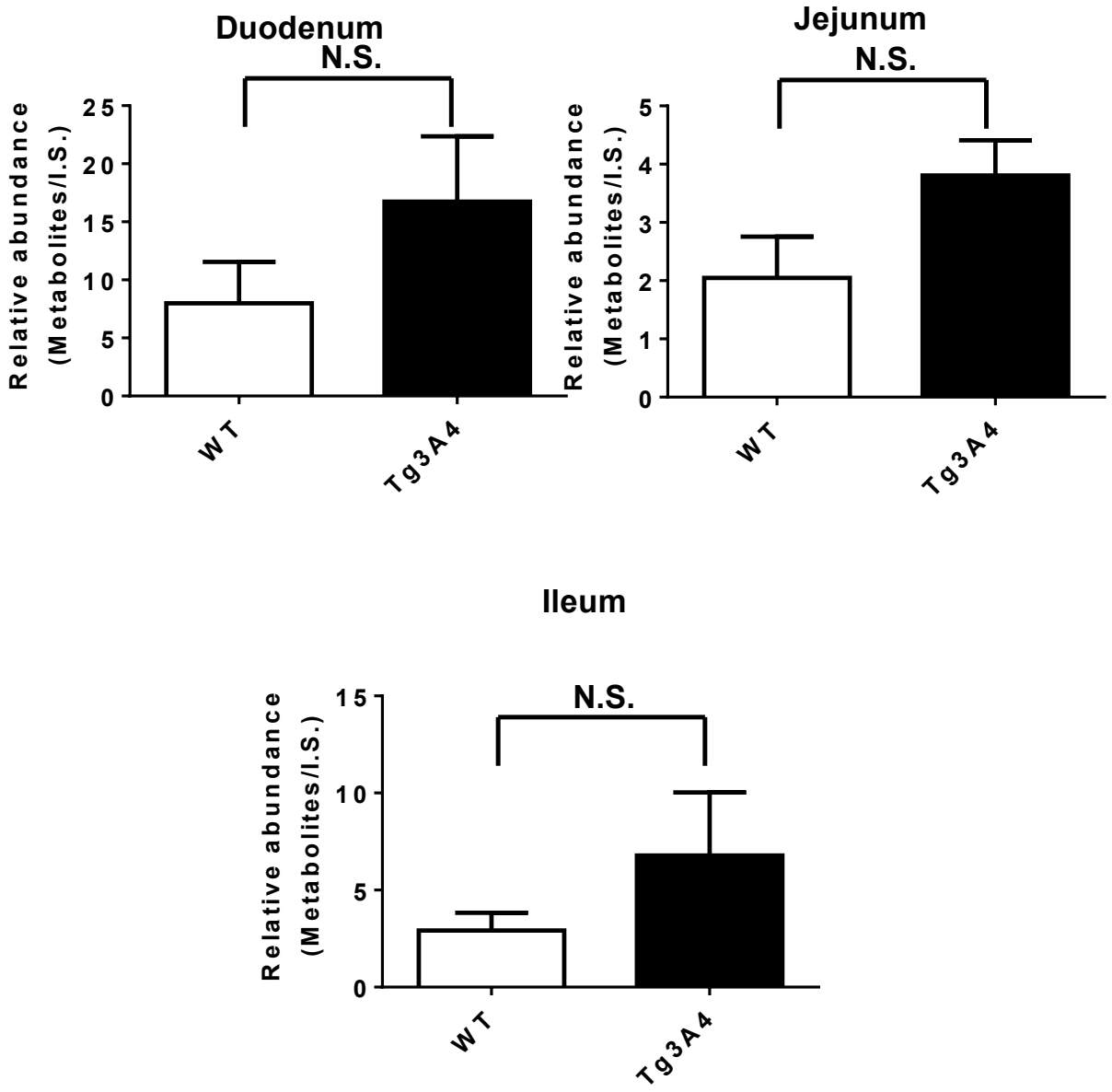


**Supplemental Figure 5.** Comparison of the relative abundance of TCA in intestine (duodenum, jejunum, and ileum) homogenates in wild-type and Tg-3A4 mice. N.S., not significant. Duo: duodenum, Jej: jejunum.

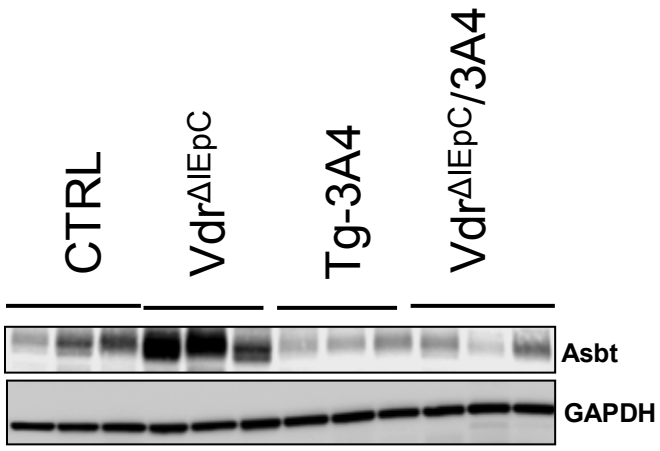


**Supplemental Figure 6.** Western blotting of ASBT expression in ileums obtained from LCA-treated control (Ctrl), *Vdr*$^{\Delta IEpC}$, Tg-3A4, and *Vdr*$^{\Delta IEpC}$/3A4 mice.